Ca^{2+}-induced Thermoreversible and Controllable Complexation of Poly(*N*-vinylcaprolactam-*co*-sodium acrylate) Microgels in Water

Shufu Peng and Chi Wu*

The Open Laboratory of Bond-selective Chemistry, Department of Chemical Physics, University of Science and Technology of China, Hefei, Anhui, China, and Department of Chemistry, The Chinese University of Hong Kong, Shatin, Hong Kong

Received: August 2, 2000; In Final Form: November 17, 2000

Spherical microgels were prepared by precipitation copolymerization of *N*-vinylcaprolactam and sodium acrylate [P(VCL-*co*-NaA)] in water at 60 °C. Because it is a thermally sensitive polymer, the increase of temperature in the range 25−40 °C leads to a continuous shrinking of the poly(*N*-vinylcaprolactum) (PVCL) chain. The copolymerization of a few molar percent of NaA into a PVCL chain increases the extent of its swelling and shifts the temperature at which it shrinks to a slightly higher level. Our results revealed that, in the shrinking process, calcium ions (Ca^{2+}) could induce a profound thermoreversible complexation of the P(VCL-*co*-NaA) microgels at a critical temperature (T_c) which was nearly independent of the NaA content. However, both the rate and degree of the complexation at T_c increased with the NaA content. A comparison of linear P(VCL-*co*-NaA) chains and spherical P(VCL-*co*-NaA) microgels in the complexation is presented.

Introduction

Recently, swelling and shrinking of hydrogels under different conditions, such as temperature, pH, composition, ionic strength, and solvent, have attracted much attention. For example, hundreds of experimental and theoretical studies on thermally sensitive poly(*N*-isopropylacrylamide) (PNIPAM) gels have been reported.[1] In general, a thermally sensitive hydrogel has a lower critical solution temperature (LCST); namely, it swells at lower temperatures but shrinks as the temperature increases. Introducing a few molar percent of hydrophobic or hydrophilic groups into a hydrogel can alter the temperature at which it shrinks and the extent of its swelling.[2−5] In contrast, reports on thermally sensitive microgels are limited, partially because their preparation and observation are relatively more difficult. Experimentally, it is important to prepare microgels with a sufficient amount of cross-linking points so that each microgel is still a swollen three-dimensional polymer network. Using microgels offers several advantages. For example, microgels can nearly instantly reach their shrinking and swelling limits in comparison with days required by bulk gels. Microgels can also be injected in some special applications.

Poly(*N*-vinylcaprolactam) (PVCL) is a relatively new type of nonionic water-soluble polymer. It was developed for hair-care and cosmetic applications. In principle, it should be more biocompatible than PNIPAM. PVCL can complex with organic compounds,[6−10] it can resist hydrolysis,[11] and its gel can undergo a continuous volume transition in the temperature range 25−36 °C.[12] Up to now, only a few studies on PVCL and its gels have been reported, partially because its polymerization is more difficult and partially because its volume transition is not as sharp as that of the PNIPAM gels. However, its biocompability led us to initiate this study to see whether PVCL microgels can be used as an injecting composition for certain biomedical applications. It is also known that a certain kind of metal ion, such as Ca^{2+}, can interact with carboxylic groups on polymer chains via a polyion/metal complexation to form interchain aggregation.[13−17] This complexation led us to think whether it can be used to immobilize microgels incorporated with a proper amount of carboxylic groups inside body after injection. This study is a fundamental research with some envisioned biomedical applications.

Materials and Methods

Materials. *N*-Vinylcaprolactam monomer (VCL, courtesy of BASF) was purified further by a reduced pressure distillation. Sodium acrylate monomer (NaA, from Lancaster) was used without further purification. Potassium persulfate as an initiator (KPS, from Aldrich) and *N*,*N*′-methylenebisacrylamide as a cross-linking agent (MBAA, from Aldrich) were recrystallized three times in methanol. Calcium chloride (anhydrous $CaCl_2$, from ACROS) was used without further purification.

Sample Preparation. Spherical poly(*N*-vinylcaprolactam-*co*-sodium acrylate) [P(VCL-*co*-NaA)] microgels were prepared by precipitation polymerization in water. Into a 150-mL three-neck flask equipped with a reflux condenser, a thermometer, and a nitrogen-bubbling tube, were added 7.3 mmol VCL monomer, a proper amount of NaA comonomer, 0.19 mmol MBAA, and 40 mL deionized water. The solution was stirred and bubbled by nitrogen for 1 h to remove oxygen before 0.045 mmol KPS aqueous solution was added to start the polymerization at 60 °C for 24 h. The resultant P(VCL-*co*-NaA) microgels were purified by a successive four-times centrifugation (Sigma 2K15 ultracentrifuge, at 15 300 rpm and 40 °C), decantation, and redispersion in deionized water to remove

* Address for correspondence: Department of Chemistry, The Chinese University of Hong Kong, Shatin, N. T., Hong Kong. E-mail: chiwu@cuhk.edu.hk.

10.1021/jp0028094 CCC: $20.00
Published on Web 03/06/2001

TABLE 1: Laser-Light−Scattering Characterization of Linear P(VCL-co-NaA) Chains and Spherical Microgels in Deionized Water

	L-P(VC L-*4.6*A)			G-P(VC L-*1.0*A)			G-P(VC L-*4.3*A)			G-P(VC L-*9.1*A)		
T (°C)	$M_w \times 10^6$ (g/mol)	$\langle R_h \rangle$ (nm)	$\langle R_g \rangle / \langle R_h \rangle$	$M_w \times 10^9$ (g/mol)	$\langle R_h \rangle$ (nm)	$\langle R_g \rangle / \langle R_h \rangle$	$M_w \times 10^9$ (g/mol)	$\langle R_h \rangle$ (nm)	$\langle R_g \rangle / \langle R_h \rangle$	$M_w \times 10^9$ (g/mol)	$\langle R_h \rangle$ (nm)	$\langle R_g \rangle / \langle R_h \rangle$
27	3.03	73	1.33	1.34	330	0.70	2.22	355	0.87	5.54	515	1.29
37	3.02	33	0.92	1.40	191	0.73	2.10	229	0.88	5.41	371	0.91
50	3.06	25	0.82	1.42	134	0.85	2.13	177	0.92	5.21	272	1.11

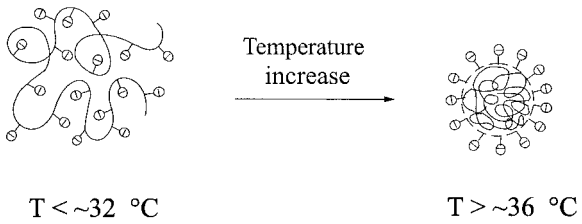

Figure 1. Schematic of the formation of a single P(VCL-*co*-NaA) chain core−shell nanostructure.

unreacted low molar mass molecules. The P(VCL-*co*-NaA) microgel dispersion obtained had a microgel concentration of $\sim 1.5 \times 10^{-2}$ g/mL, which was diluted with deionized water to concentrations lower than $\sim 1 \times 10^{-5}$ g/mL for laser-light-scattering measurements. Note that the polymer chains are cross-linked inside microgels so that the dilution did not lead to dissolution of the polymer chains. The microgels with different contents of NaA were labeled as P(VCL-*m*A), where "*m*" represents the average molar content of acrylic groups. Linear P(VCL-*co*-NaA) chains were prepared in a similar way without adding the cross-linking agent, MBAA.

Methods. The details of our laser-light-scattering (LLS) spectrometer can be found elsewhere.[18] In static LLS, the angular dependence of the absolute excess time-averaged scattered intensity, known as the Rayleigh ratio $R_{vv}(q)$, can lead to the weight-average molar mass (M_w), the z-average root-mean-square radius of gyration $\langle R_g^2 \rangle^{1/2}$, or written as $\langle R_g \rangle$), and the second virial coefficient (A_2), where q is the scattering vector. In dynamic LLS, the cumulant or Laplace inversion analysis of the measured intensity−intensity time correlation function $G^{(2)}(q,t)$ in the self-beating mode can result in an average line width ($\langle \Gamma \rangle$) or a line width distribution [$G(\Gamma)$].[19,20] For a pure diffusive relaxation, Γ is related to the translational diffusion coefficient D by $(\Gamma/q^2)_{C \to 0, q \to 0} = D$ and to the hydrodynamic radius (R_h) by the Stokes−Einstein equation, $D = k_B T/(6\pi\eta R_h)$, where k_B, T, and η are the Boltzmann constant, the absolute temperature, and the solvent viscosity, respectively.[21]

Results and Discussion

Table 1 summarizes static and dynamic LLS results of linear P(VCL-*co*-NaA) chains and spherical microgels with different contents of NaA in the absence of Ca^{2+} in the swollen (27 °C) and collapsed (50 °C) states. In each case, M_w is independent of the temperature, indicating no interchain or no interparticle aggregation. As expected, linear chain has a larger change in $\langle R_h \rangle$ than microgels. For linear chains, the decrease of $\langle R_g \rangle / \langle R_h \rangle$ from 1.33 to 0.82 indicates a coil-to-globule transition of the chain conformation, presumably leading to a single-chain core−shell nanostructure or a single-chain micelle, as shown in Figure 1. On the other hand, the shrinking of the microgels as the temperature increases was relatively smooth, similar to the temperature-induced volume change of neutral PVCL microgels.[12] However, the ionic groups make the PVCL chain more hydrophilic, which leads to a greater extent of swelling

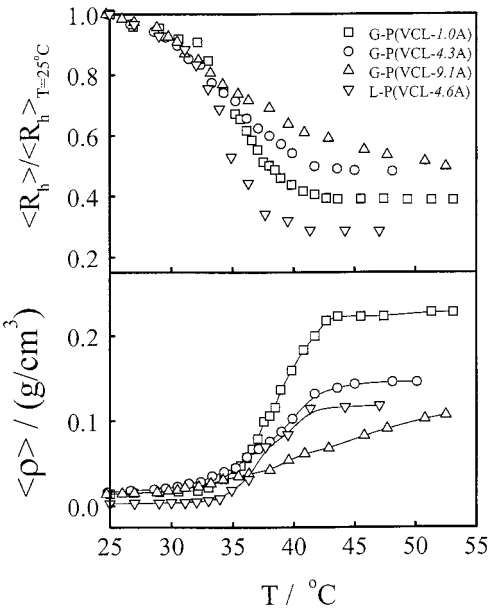

Figure 2. Temperature dependence of the relative average hydrodynamic radius $\langle R_h \rangle / \langle R_h \rangle_{T=25°C}$ and the average chain density $\langle \rho \rangle$ for the linear P(VCL-*co*-NaA) chains and spherical microgels copolymerized with different amounts of NaA, where $\langle R_h \rangle_{T=25°C}$ is the average hydrodynamic radius $\langle R_h \rangle$ at 25 °C.

at lower temperatures, shifts the temperature at which the microgels shrink to a higher level, and results in a less compact globule.[22,23] The increase of $\langle R_g \rangle / \langle R_h \rangle$ as the ionic content increases indicates further swelling of the microgels.

Figure 2 clearly shows that the shrinking of the linear chains is more than that of the microgels. The relative shrinking of the microgels decreases as the ionic content increases. Note that in the temperature range studied, there was no change in M_w in each case, that is, no intermicrogel aggregation in the shrinking process. Figure 2 also shows a better view of the shrinking of the linear chains and microgels in terms of the average chain density ($\langle \rho \rangle$) defined as $M_w/[(4/3)\pi \langle R_h \rangle^3]$. In both the swollen and collapsed states, the linear chains have a lower density than the microgels, because the cross-linking limits the swelling of the gel network. Except for the microgels with the highest ionic content, both the linear chains and microgels reached their corresponding collapsed states at 42 °C. The slow increase of $\langle \rho \rangle$ for the P(VCL-*9.1*A) microgels can be attributed to a balance between strong electrostatic repulsion and hydrophobic attraction. If using $\langle \rho \rangle$ at 25 °C as a reference, we found that $\langle \rho \rangle$ increased ~40 times for the linear chains but only 8−16 times for the microgels, depending on the ionic content.

Figure 3 shows a completely different picture of the temperature dependence of the average hydrodynamic radius ($\langle R_h \rangle$) and the apparent weight-average molar mass ($M_{w,app}$) of the linear chains and microgels in 0.03 M $CaCl_2$ aqueous solution. In the range 25−31.8 °C, the microgels shrink as the temperature increases, but $M_{w,app}$ is independent of the temperature, indicating no intermicrogel aggregation. At the transition temperature

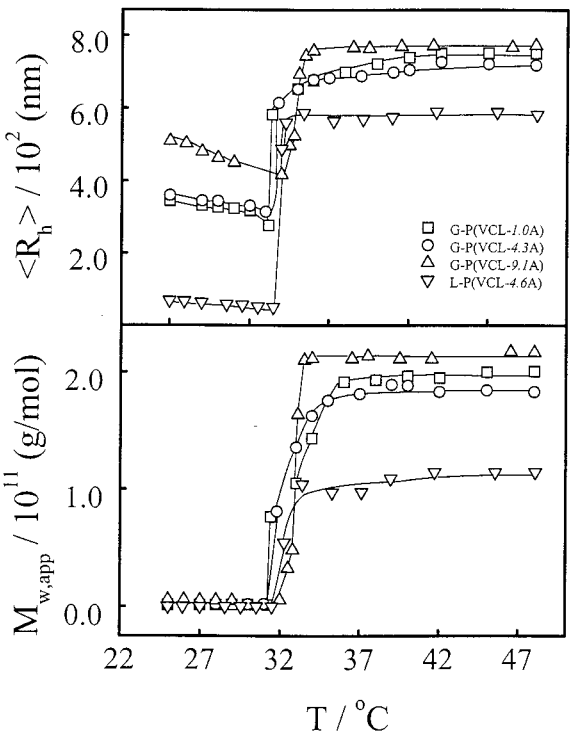

Figure 3. Temperature dependence of the average hydrodynamic radius $<R_h>$ and the apparent weight-average molar mass ($M_{w,app}$) of linear P(VCL-*co*-NaA) chains and spherical microgels in the presence of Ca^{2+}, where $[Ca^{2+}] = 0.03$ M.

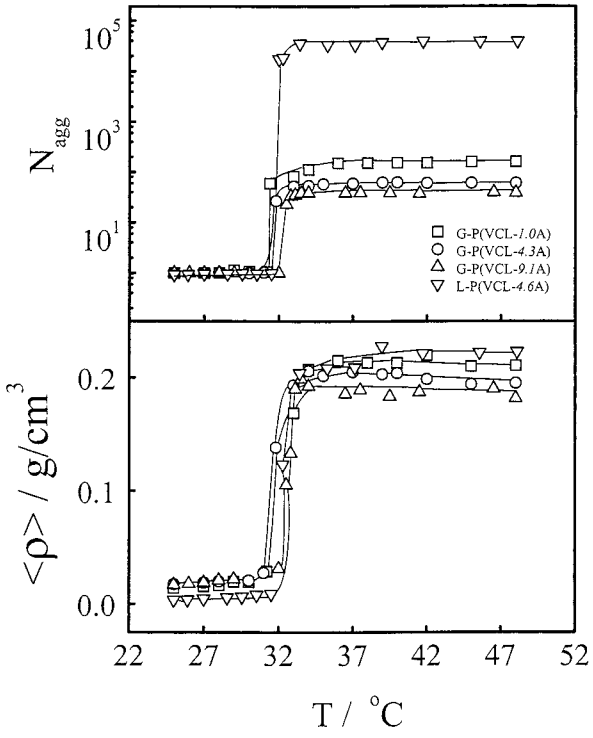

Figure 4. Temperature dependence of the average number of aggregation (N_{agg}) and the average chain density $<\rho>$ of linear P(VCL-*co*-NaA) chains and spherical microgels in the presence of Ca^{2+}, where $[Ca^{2+}] = 0.03$ M.

($T_c \sim 32$ °C), the average hydrodynamic size and the apparent weight-average molar mass sharply increase, revealing a clear intermicrogel aggregation. Note that the aggregation of both linear chains and spherical microgels stops when the temperature is higher than ~36 °C, clearly showing the existence of the mesoglobular phase in a dilute heteropolymer solution.[24−26]

Figure 4 shows that for the linear chains, the average number of the chains inside each complex particle (N_{agg}) is as high as $\sim 4 \times 10^4$; whereas for the microgels, N_{agg} is much less, only in the range 40−200, where N_{agg} is defined as $M_{w,app}/M_w$ and M_w is the weight-average molar mass of linear chains or spherical microgels. This is because linear chains can entangle and complex with each other through the interaction between Ca^{2+} and −COO− to form a hyperbranched structure. Whereas for the microgels, when the temperature reaches T_c, the collapse of PVCL chains forces the hydrophilic −COO− groups to stay on the periphery of the microgel. The complexation between Ca^{2+} and −COO− sticks different microgels together. The fact that the complexation occurred in a narrow temperature range suggests that the intermicrogel aggregation is related to the transition of PVCL chains from hydrophilic to hydrophobic.

Figure 4 also shows that the resultant complexes have a similar average chain density $<\rho>$ of ~0.2 g/cm^3 despite a big difference in N_{agg}. A slight decrease of $<\rho>$ with increasing ionic content occurs because the chains with more ionic groups are more hydrophilic and collapse less at high temperatures. The higher $<\rho>$ of the linear chains is related to the chain entanglement. Note that both the linear chains and the microgels have an amphiphilic character at higher temperatures. The shrinking of each linear chain forces most of the ionic groups to form a relatively more hydrophilic periphery, similar to a micelle,[27−30] whereas in the microgels, most of the ionic groups are trapped inside the microgel because of the cross-linking. There are thus fewer chances to form the intermicrogel complexes, which explains why N_{agg} (microgel) is much lower than N_{agg} (linear chain) and why N_{agg} (microgel) decreases as the ionic content increases.

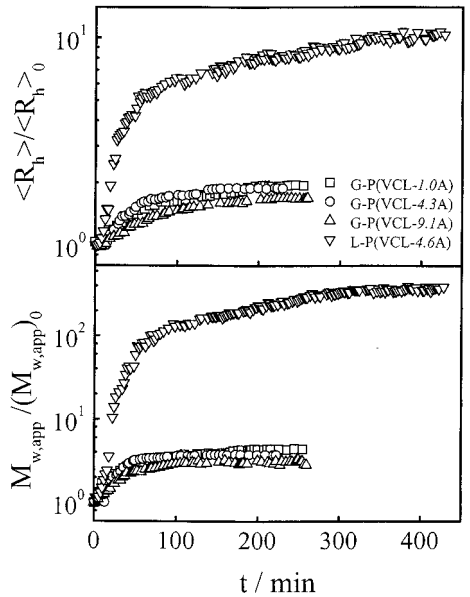

Figure 5. Time dependence of the relative average hydrodynamic radius ($<R_h>/<R_h>_0$) and relative weight-average molar mass [$M_{w,app}/(M_{w,app})_0$] of linear P(VCL-*co*-NaA) chains and spherical microgels in the presence of Ca^{2+} at $T = 32$ °C, where $<R_h>_0$ and $(M_{w,app})_0$ are the average hydrodynamic radius $<R_h>$ and the apparent weight-average molar mass $M_{w,app}$ at $t = 0$.

Figure 5 shows the time dependence of the relative average hydrodynamic radius $<R_h>/<R_h>_0$ and the relative apparent weight-average molar mass [$M_{w,app}/(M_{w,app})_0$] of the P(VCL-*co*-NaA)/Ca^{2+} complexes with different NaA contents, where the subscript "0" means the values at $t = 0$. The P(VCL-*9.1*A) microgels have lower ratios of $<R_h>/<R_h>_0$ and $M_{w,app}/(M_{w,app})_0$, because more ionic groups inside the gel network

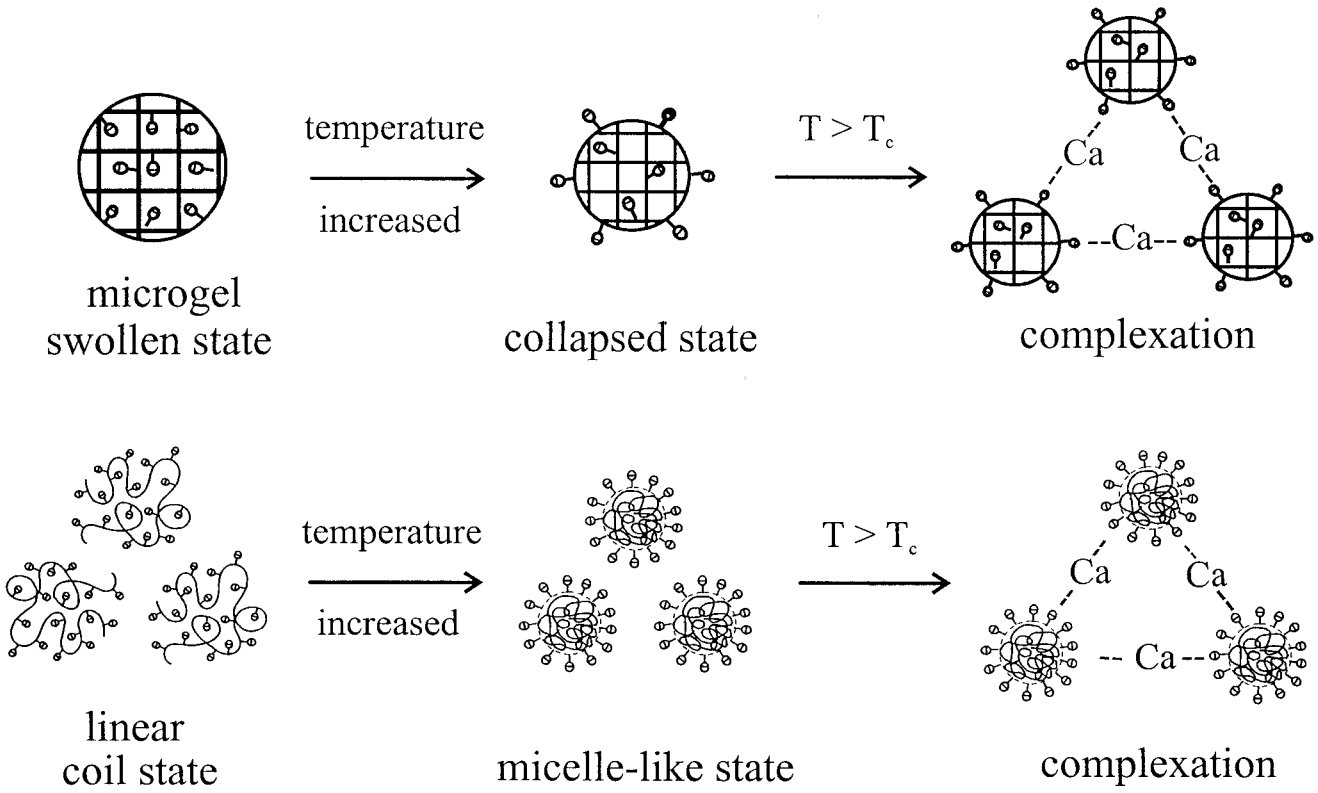

Figure 6. Schematic of the temperature dependence of linear P(VCL-*co*-NaA) chains and spherical microgels in the presence of Ca^{2+}.

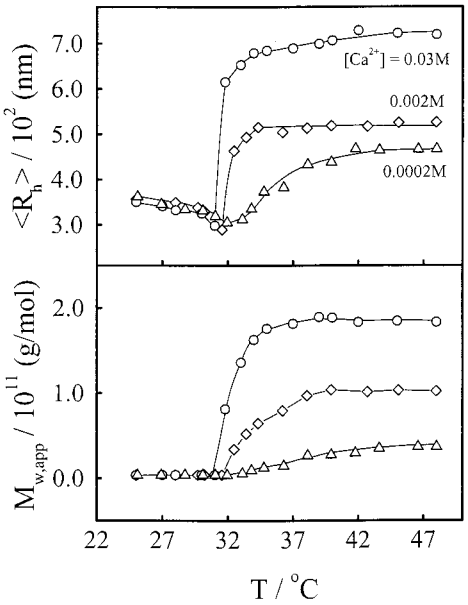

Figure 7. Temperature dependence of the average hydrodynamic radius $<R_h>$ and apparent weight-average molar mass ($M_{w,app}$) of G−P(VCL-*4.3*A) microgels with different Ca^{2+} concentrations.

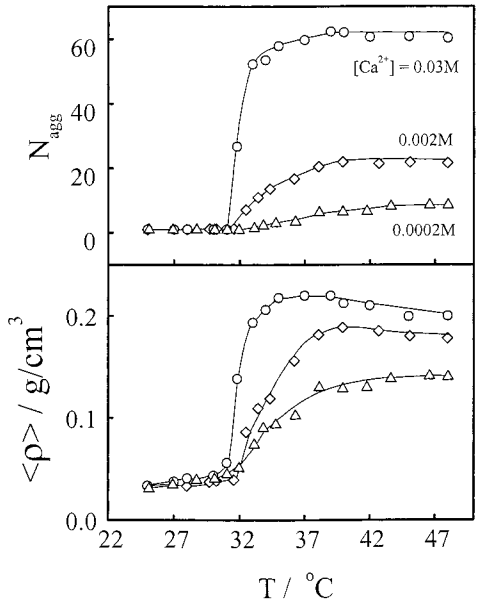

Figure 8. Temperature dependence of the average number of aggregation (N_{agg}) and the average chain density $<\rho>$ of G−P(VCL-*4.3*A) microgels with different Ca^{2+} concentrations.

prevent the shrinking of the microgel due to electrostatic repulsion, leading to less complexation with Ca^{2+}. For the linear chains, both $<R_h>/<R_h>_0$ and $M_{w,app}/(M_{w,app})_0$ are much larger than those for the microgels, clearly indicating that the linear chains can entangle and complex with each other via the interaction between Ca^{2+} and −COO− to form a branched structure. Figure 6 shows a schematic of the complexation, induced via an interaction between Ca^{2+} and −COO−.

Figure 7 shows the temperature dependence of the average hydrodynamic radius $<R_h>$ and the apparent weight-average molar mass ($M_{w,app}$) for P(VCL-*4.3*A) microgels in the presence of different amounts of Ca^{2+}. The complexation occurs at a similar temperature despite a variation of Ca^{2+} concentration, but both $<R_h>$ and $M_{w,app}$ increase as $[Ca^{2+}]$ increases. The increase of the ionic content has little effect on $<R_h>$. Figure 8 shows that the average number of the microgels inside each intermicrogel complex (N_{agg}) are ∼60, ∼20, and ∼8, respectively, for $[Ca^{2+}] = 3 \times 10^{-2}$ M, 2×10^{-3} M, and 2×10^{-4} M. The average chain density $<\rho>$ of the complexes decreases as N_{agg} decreases, maybe because of an imperfect packing of larger microgels inside each complex, especially when each complex is only made of about eight microgels.

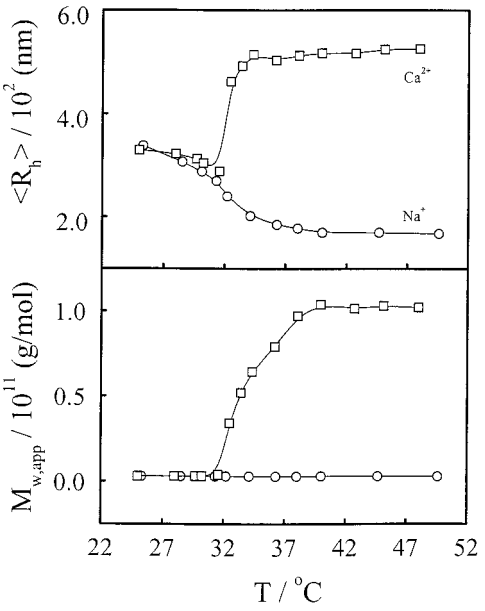

Figure 9. Temperature dependence of the average hydrodynamic radius $<R_h>$ and the apparent weight-average molar mass ($M_{w,app}$) of G−P(VCL-*4.3*A) microgels in the presence of Na^+ and Ca^{2+}, respectively, where $[Ca^{2+}] = 0.002$ M, $[Na^+] = 0.004$ M.

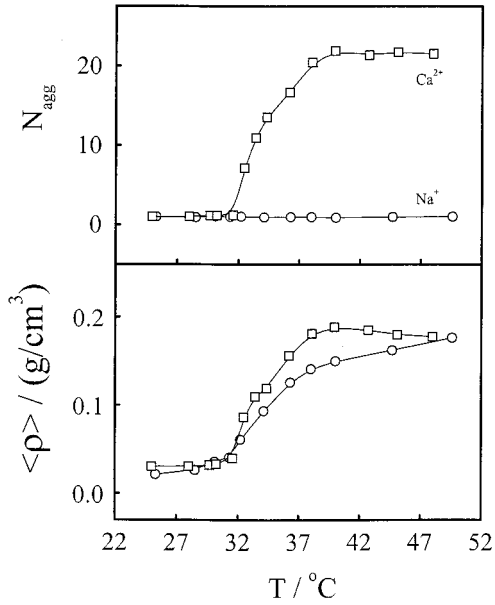

Figure 10. Temperature dependence of the average number of aggregation (N_{agg}) and the average chain density $<\rho>$ of G−P(VCL-*4.3*A) microgels in the presence of Na^+ and Ca^{2+}, respectively, where $[Ca^{2+}] = 0.002$ M, $[Na^+] = 0.004$ M.

Figures 9 and 10 show the effect of monovalent and divalent ions on the complexation of microgels. In the presence of Na^+, $<R_h>$ and $<\rho>$ gradually decrease as the temperature increases, but neither $M_{w,app}$ and N_{agg} change, indicating that there is no intermicrogel aggregation. The shrinking of individual microgels is due to the intramicrogel hydrophobic attraction. This is understandable because the presence of monovalent Na^+ can only increase the ionic strength and reduces electrostatic repulsion between carboxylic groups. Besides the influence on the ionic strength, divalent Ca^{2+} can pull two carboxylic groups together so that Ca^{2+} can induce both the intermicrogel and intramicrogel complexation.

Conclusions

The copolymerization of a few molar percent of ionic NaA into the P(VCL-*co*-NaA) microgel can slightly raise its volume transition temperature and increase the extent of its swelling. At the transition temperature (∼32 °C), the PVCL chains become hydrophobic and insoluble. The collapse of the PVCL chains forces the −COO− groups to stay on the periphery. The intramicrogel complexation between Ca^{2+} and these $-COO^-$ groups leads to the shrinking of microgels, but the intermicrogel complexation induces the aggregation. The aggregation temperature is independent of the cationic content, revealing that the aggregation is controlled by the hydrophilicity of the PVCL chains. A comparison of linear copolymer chains and spherical microgels showed that the aggregation of linear chains is much more profound than that of spherical microgels, presumably because of the competition between the inter- and intrachain complexation. The domination of the intrachain complexation (the cross-linking inside each microgel can be viewed as the intrachain process) leads to less aggregation. As expected, the extent of the complexation increases as the Ca^{2+} concentration increases.

Acknowledgment. Financial support of the Bai Ren Project, NNSFC29974027 and of the Research Grants Council of the Hong Kong Special Administration Region Earmarked Grant 1999/2000 (CUHK 4209/99P, 2160122) is gratefully acknowledged.

References and Notes

(1) Sat, S.; Kong, M.; Inmate, H. *Adv. Polym. Sci*. **1993**, *109*, 207.
(2) Beltran, S.; Baker, J. P.; Hooper, H. H.; Blanch, H. W.; Prausnitz, J. M. *Macromolecules* **1991**, *24*, 549.
(3) Zhou, S.; Chu, B. *J. Phys. Chem. B* **1998**, *102*, 1364.
(4) Snowden, M. J.; Chowdhry, B. Z.; Vincent, B.; Morris, G. E. *J. Chem. Soc., Faraday Trans*. **1996**, *92*(24), 5013.
(5) Yoo, M. K.; Sung, Y. K.; Lee, Y. M.; Cho, C. S. *Polymer* **2000**, *41*, 5713.
(6) Pashkin, I. I.; Kirsh, Yu. E.; Zubov, V. P.; Anisimova, T. V.; Kuzkina, I. F.; Voloshina, Ya. V. *Polym. Sci., Ser. A* **1993**, *35*, 581.
(7) Shestyuk, S. F.; Galaev, I. Yu.; Savitskii, A. P.; Kirsh, Yu. E.; Berezin, I. V. *Biothechnologiya 3* **1987**, *2*, 178.
(8) Eisele, M.; Burchard, W. *Makromol. Chem*. **1990**, *191*, 169.
(9) Kirsh, Yu. E.; Galaev, I. Yu.; Karaputadze, T. M.; Margolin, A. A.; Shvyadas, V. K. *Biothechnologiya* 3 **1987**, *2*, 184.
(10) Solomon, O. F.; Corciovei, M.; Boghina, C. *J. Appl. Polym. Sci*. **1968**, *12*, 1843.
(11) Makhaeva, E. E.; Thanh, L. T. M.; Starodoudoubtsev, S. G.; Khokhlov, A. R. *Macromal. Chem. Phys*. **1996**, *197*, 1973.
(12) Mikheeva, L. M.; Grinberg, N. V.; Mashkevich, A. Ya.; Grinberg, V. Ya. *Macromolecules* **1997**, *30*, 2693.
(13) Jordan, D. S.; Green, D. W.; Terry, R. E.; Willhite, G. P. *J. Soc. Pet. Eng.* **1982**, *8*, 463.
(14) Flory, P. J.; Osterheld, J. E. *J. Phys. Chem*. **1954**, *58*, 653.
(15) Ohmine, I.; Tanaka, T. *J. Chem. Phys*. **1982**, *77*, 5725.
(16) Ben Jar, P. Y.; Wu, Y. S. *Polymer* **1997**, *38*, 2557.
(17) Peng, S.; Wu, C. *Macromolecules* **1999**, *32*, 585.
(18) Wang, X.; Xu, Z.; Wan, Y.; Huang, T.; Pispas, S.; Mays, J. W.; Wu, C. *Macromolecules* **1997**, *30*, 7202.
(19) Berne, B. J.; Pecora, R. *Dynamic Light Scattering*; Plenum Press: New York, 1976.
(20) Chu, B. *Laser Light Scattering*, 2nd ed.; Academic Press: New York, 1991.
(21) Stockmayer, W. H.; Schmidt, M. *Pure Appl. Chem*. **1982**, *54*, 407.
(22) Hirokawa, Y.; Tanaka, T. *J. Chem. Phys*. **1984**, *81*, 6379.
(23) Otake, K.; Inomata, H.; Konno, M.; Saito, S. *J. Chem. Phys*. **1989**, *91*, 1345.
(24) Timoshenko, E. G.; Kuznetsov, Y. A.; Dawson, K. A. *Phys. Rev. E*. **1998**, *57*, 6801.
(25) Khokhlov, A. R.; Khalatur, P. G. *Phys. Rev. Lett*. **1999**, *82*, 3456.
(26) Virtanen, J.; Baron, C.; Tenhu, H. *Macromolecules* **2000**, *33*, 336.
(27) Shibayama, M.; Tanaka, T.; Han, C. C. *J. Chem. Phys*. **1992**, *97*, 6829.
(28) Li, Y.; Tanaka, T. *J. Chem. Phys*. **1989**, *90*, 5161.
(29) Annaka, M.; Tanaka, T. *Nature* **1992**, *355*, 430.
(30) Zeldovich, K. B.; Dormidontova, E. E.; Khokhlov, A. R. *J. Phys. II* **1997**, *7*, 627.